A&A 373, 987–992 (2001)
DOI: 10.1051/0004-6361:20010567

Astronomy & Astrophysics

Non-LTE gallium abundance in HgMn stars⋆

M. Zboril[1] and K. A. Berrington[2]

[1] Astronomical Institute, Tatranská Lomnica, SK-059 60, Slovakia
[2] School of Science and Mathematics, Sheffield Hallam University, Sheffield, S1 1WB, UK

Received 5 January 2000 / Accepted 19 April 2001

Abstract. We present, for the first time, the Non-LTE gallium equivalent widths for the most prominent gallium transitions as identified in real spectra and in (hot) mercury-manganese star. The common feature of the departure coefficients is to decrease near the stellar surface, the collision rates are dominant in many cases and the Non-LTE equivalent widths are generally smaller. In particular, the abundance difference as derived from UV and visual lines is reduced. The photoionization cross sections were computed by means of standard R-matrix formalism.

Key words. stars: abundances – stars: atmospheres – stars: chemically peculiar

1. Introduction

The upper main sequence of the H-R diagram is populated by a number of chemically peculiar (CP) stars. At present there are several groups of CP stars encompassing spectral types from early F through early B and characterized variously by intense magnetic fields, unusually slow rotation, rapid oscillations, photometric and spectroscopic variability and surface abundances usually departing from the solar pattern by many orders of magnitude.

In this contribution we will deal with CP3 subgroup, i.e. Hg-Mn stars. These stars have either very weak magnetic field (a few hundred Gauss) or complex structures (Landstreet 1982). There are no spectrum variabilities detected as yet and probably no light variabilities as well (e.g. Zboril & Budaj 1993; Zboril & Budaj 1999; Adelman 1998). The most recent LTE calculations (Dworetsky et al. 1998) for Ga demonstrated that the discrepancies in (LTE) abundances deduced by previous workers (e.g. Lanz et al. 1993; Takada-Hidai et al. 1986), between UV resonance lines and optical lines, were largely due to ignoring the effects of hyperfine structure and blends of the optical lines. Specifically, they showed that discrepancies in gallium abundance as derived from UV and optical lines is reduced to 0.2 dex, where 0.1 dex is due to simplified approximation to the true hyperfine structure and remaining 0.1 dex can probably be accounted for by the stratification of gallium in the stellar atmosphere.

Here we study Non-LTE (also NLTE) gallium abundance to investigate its impact to the basic characteristics of CP3 stars: abundance, its wavelength dependence, line forming regions, expected vertical gallium stratification to support the diffusion process or otherwise and proper processes associated with gallium transitions (collisions, photoionization etc.).

2. Surface abundances

HgMn stars are characterized by a variety of overabundant elements including mercury, manganese, phosphorus and gallium (e.g. Smith & Dworetsky 1993; Smith 1994, 1996, 1997; Jomaron et al. 1999; Woolf & Lambert 1999). Mercury exhibits star-to-star variations in its *isotopic* composition which are correlated with effective temperature. Thanks to the IUE launch the new prominent ultraviolet resonance lines were analyzed and studied bringing additional information to the photospheric abundance pattern: nitrogen, aluminium and zinc were found to be largely underabundant as had been suspected from optical spectra, while copper was found overabundant in nearly all HgMn stars. Comprehensive analyses of the iron peak elements gave a complex picture: star-to-star variations seems to be real characteristics for the HgMn stars. The behaviour of light elements such as beryllium and boron is a puzzle as well, varying from "rich" status up to essentially normal one. Thus HgMn stars are a subgroup

Send offprint requests to: M. Zboril, e-mail: zboril@ta3.sk

⋆ The gallium cross-sections are only available in electronic form at the CDS via anonymous
ftp to cdsarc.u-strasbg.fr (130.79.128.5) or via
http://cdsweb.u-strasbg.fr/cgi-bin/qcat?J/A+A/373/987

of chemically peculiar stars displaying a variety of abundances even for the same chemical element.

3. The radiative diffusion model in CP3 stars

It is now generally accepted that the radiative diffusion model for CP stars suggested by Michaud (1970) can explain at least qualitatively the abundance pattern in CP stellar atmospheres. The central hypothesis of the radiative diffusion model is that sufficiently *quiescent* stellar atmospheres become chemically differentiated via the microscopic migration of elements under the competing influences of gravitational acceleration and radiation pressure. As CP3 stellar atmospheres are believed uncomplicated by surface magnetic fields, rotation or turbulence and thus diffusion should operate in its "purest" form (parameter-free model Michaud 1981, 1986).

The scenario for development of HgMn stars is the following: chemical differentiation of the atmosphere is triggered by the disappearance of a relatively deep HeII convective zone after about 3×10^6 yr. This time scale agrees very well with the age of the youngest clusters where HgMn stars are observed. Detailed radiative acceleration calculations have been performed to derive the maximum abundance that can be supported by the radiation field in an atmosphere. Large temperature dependent overabundances are predicted for Mn and Ga while Mg and Si are expected to be supported at abundances within a factor 5–10 of their solar values. This figure is in very good agreement with IUE observations except for Be where in some stars Be II resonance lines suggest rather normal abundance and the overabundance is predicted.

Note that for other CP stars the radiative acceleration calculations need to involve more physical aspects such as magnetic field or, the case of He-rich stars, stellar wind, otherwise He would completely sink in He-rich stellar atmospheres.

4. Gallium radiative acceleration

Following the original Michaud's suggestion, several authors developed depth dependent radiative accelerations and vertical stratification of some elements in the atmospheres of CP stars. One of the interesting calculations for gallium are those of Budaj et al. (1993). It is important to understand that radiative acceleration $g_i^{\rm rad}$ is depth dependent and needs to be evaluated by summing at least all bound-bound and bound-free transitions at every depth point in the stellar atmosphere. Solving the equations for depth dependent gallium radiative acceleration and elemental concentration in stellar atmosphere, Budaj et al. (1993) found a steep gradient for gallium abundance for a star having $T_{\rm eff} = 12\,000$ K and $\log g = 4.0$. This solution, i.e. gallium abundance distribution was later compared with the schematic stratification model derived empirically for HR 7143 (Smith 1995) using co-added high resolution IUE spectra and resonance Ga II and GaIII transitions. The agreement between theoretical and empirical abundance distribution is encouraging, though theoretical result has still some simplifications.

5. Gallium model atom

One such simplification was the LTE approximation involved and in this contribution we pay attention to the Non-LTE option and its impact to the gallium abundance in HgMn stars. To illustrate the problem let's consider the bound-bound absorption coefficient expression

$$k_\nu^{\rm line} = cb_i \frac{N_{\rm ion}}{U_{\rm ion}} \left(1 - \frac{b_i}{b_j} {\rm e}^{-h\nu/kT}\right) {\rm e}^{-E_i/kT} H(a,v)/\triangle\nu_{\rm D}(1)$$

where c is appropriate constant, b_i, b_j NLTE departure coefficients, $H(a,v)$ Voigt function, $\triangle\nu_{\rm D}$ Doppler halfwidth, E_i excitation potential of lower level, $N_{\rm ion}, U_{\rm ion}$ ion concentration and partition function respectively. A further quantity is the total source function in radiative transfer equation (Sect. 8).

Now, if the NLTE departure coefficients do not equal to unity, the line absorption coefficient has a different value with respect to LTE option and subsequently solving radiative transfer equation (optical depth depends on total absorption coefficient) one may get a new set of intensities and therefore different measurable quantities such as anomalous curve-of-growth behaviour, line profiles and equivalent widths. NLTE departure coefficients are abundance dependent as well. It is therefore desirable to examine how this situation can influence the vertical abundance distribution of the chemical element.

5.1. Total levels number

To perform NLTE computations for gallium we took 14 explicit levels for Ga I ion, 16 levels for Ga II, 3 levels for Ga III and 1 level for Ga IV. The abbreviation "explicit" has the meaning that NLTE populations are to be computed. Table 1 offers the gallium atomic structure, designation and excitation energy.

Finally, we note that Ga I contribution is small, as this neutral state is weakly populated and has rather weak lines. All close energy states (typically 0.1 eV) were lumped together and treated as single level.

5.2. Cross-sections, radiative and collisional rates

The electronic configuration of gallium, $1s^2 2s^2 2p^6 3s^2 3p^6 4s^2 3d^{10} 4s^2$ 4p, is the configuration of boron-like atoms due to valence electron in *p shell*. If ground state of neutral gallium is controlled by photoionization, photons with $\lambda < 2070$ Å, it is desirable to know photoionization cross section for this level to evaluate properly excited levels being populated by recombination from GaII following photoionization of the ground state. Ground states of next higher ions, Ga II and GaIII, would involve extreme UV radiation, photons with $\lambda < 600$ Å, being thus competitive with HeI ground state. Extreme UV and X-ray emissions

Table 1. Ga level structure.

ion	desig.	n	E (Ry)
Ga I	4p2P	4	0.0
Ga I	4s2S	4	0.22417
Ga I	5p2P	5	0.29777
Ga I	4d2D	4	0.31500
Ga I	5s2S	5	0.33846
Ga I	4p4P	4	0.35454
Ga I	6p2P	6	0.36363
Ga I	5d2D	5	0.36839
Ga I	4f2F	4	0.37282
Ga I	6s2S	6	0.37957
Ga I	7p2P	7	0.39120
Ga I	6d2D	6	0.39295
Ga I	5f2F	5	0.39555
Ga I	5g2G	5	0.39588
Ga II	4s2 1S	4	0.0
Ga II	4p3P	4	0.42488
Ga II	4p1P	4	0.64410
Ga II	5s3S	5	0.92045
Ga II	5s1S	5	0.95485
Ga II	4p1D	4	0.94858
Ga II	4d3D	4	1.01450
Ga II	4p3P	4	1.04496
Ga II	5p3P	5	1.05977
Ga II	5p1P	5	1.07803
Ga II	5p1D	5	1.13505
Ga II	6s3S	6	1.18956
Ga II	6s1S	6	1.19918
Ga II	5d3D	5	1.22605
Ga II	4f3F	4	1.22639
Ga II	4f1F	4	1.22662
Ga III	4s2S	4	0.0
Ga III	4p2P	4	0.57581
Ga III	5s2S	5	1.23594
GaIV	3d10 1S	3	0.0

from CP stars have been reported only for He-rich, He-weak and Si (i.e. CP2) stars (Drake et al. 1994; Babel & Montmerle 1997) and associated with stellar wind, magnetic fields and wind-shocks. Nothing has been reported on HgMn stars from which we conclude that emissions are of lower order in comparison with reported chemically peculiar stars.

The final state resolved photo-ionization cross-sections for gallium were computed with standard R-matrix formalism (Berrington et al. 1995) and Ga I ground state is displayed together with boron and aluminium ground states in Fig. 1. Basically the gallium photo-ionization cross sections possess many resonances. The R-matrix calculations are carried out in LS coupling using the close-coupling approach of scattering theory, by defining an N-electron "target" (the final photoionized states) and forming $N+1$ electron initial states from the target + electron wavefunction. Specifically, we use a 19 state Ga II target ($3d^{10}$ $4s^2$, 4s4p, 4s5s, 4s4d, $4p^2$ and $3d^9$ $4s^2$4p), a 5 state Ga III target ($3d^{10}$ 4s, 4p and $3d^9$ $4s^2$, 4s4p), a 3-state Ga IV target ($3d^{10}$ and $3d^9$4s), and a 1 state Ga V target ($3d^9$). Photoionization cross sections are

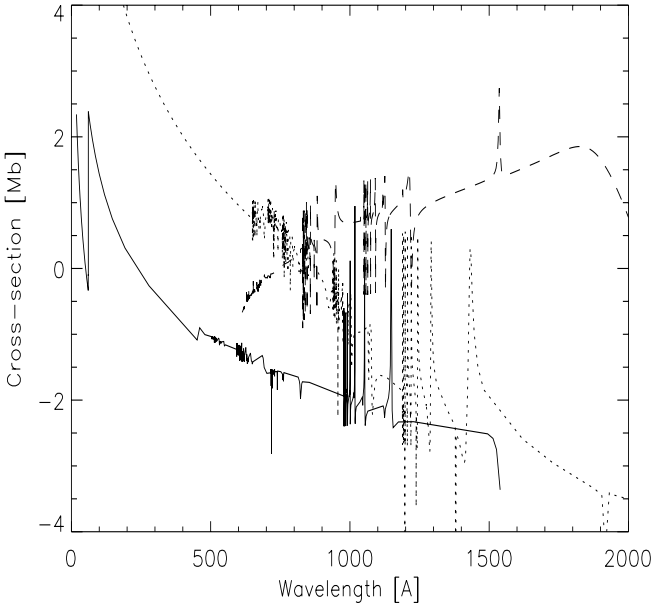

Fig. 1. Logarithm of photo-ionization cross sections from ground states of GaI, B I and Al I (from TOPBASE) in wavelength domain. The legend: **solid** line-B I ion, **dotted** line-Al I ion and **dashed** line-Ga I ion.

calculated to each of these final target states from initial ground and excited states for Ga I through Ga IV. The background cross section is primarily due to ionizing the outer electron. Resonance structure arise from autoionizing Rydberg states below each final target state. Further enhancement arises when the photon has sufficient energy to eject a 3d electron which occurs at the threshold of the $3d^9$ final states. The photoionization cross sections, which we tabulate over a fine energy mesh over the low energy region, should therefore reliably contain the main physics at these energies for the Ga ions.

For the other explicit levels of other explicit elements we refer to the Tlusty manual and input files (Hubeny et al. 1994), in other words we used the formulas being either universal or widely used and, in addition, are already coded in original software (see below).

The evaluation of collisional rates for all explicit levels was controlled by using such options as van Regemorter and Eissner-Seaton formulae for excitation and standard Allen and Seaton formulae for ionization in complete statistical equilibrium equations. The reader is referred to the program manual (Hubeny et al. 1994) for these and other expressions. We found that the NLTE level populations of explicit levels were essentially insensitive to these switches.

5.3. Complete linearization/ALI transitions

We consider two options for radiative rates as described in the Tlusty manual. In *option* 11 the transitions were treated fully explicitly which means that the radiative rates in the transition were primarily linearized. In other words the transition is represented by a set of frequencies

being included in explicit frequencies and the mean intensities of these frequencies will appear in a vector used in the complete linearization process. In *option* 22 the transitions were treated as primarily ALI transitions.

Table 2. Ratio of collisional and radiative rates in typical atmosphere depth points.

line [Å]	ID	log(DM) [g/cm^2]	u/d	d	col
2945	10	–4.3	3.0	0.005	0.02
—	46	–1.1	0.97	0.050	0.12
—	64	1.0	1	1	1
1414	10	”	1.1	3.e-5	8.0e-5
—	46	”	1	4.0e-3	7.0e-3
—	64	”	1	1	1
6334	10	”	1.2	0.06	0.25
—	46	”	0.96	0.20	0.55
—	64	”	1	1	1
4262	10	”	1.5	0.02	0.08
—	46	”	0.9	0.04	0.3
—	64	”	1	1	1
1495	10	”	3.4	7.0e-5	2e-4
—	46	”	1	6.0e-3	0.01
—	64	”	1	1	1
1534	10	”	3.5	1.0e-4	3e-4
—	46	”	1	7.0e-3	0.01
—	64	”	1	1	1

6. Model atmosphere

Model atmosphere was considered semi-empirically, i.e. with given T-τ relation, more specifically, we took this relation from LTE Kurucz's models (e.g. Kurucz 1979). The reasoning for this is fact that these models are applicable for CP3 stars and adopting the given temperature structure reduces dramatically number of iterations in modelling. This is justified since the gallium abundance is unlikely to change the temperature structure of the atmosphere.

As a next step we considered some explicit levels: 9 lowest levels of H and 1 level of HII, 14 levels of HeI and 1 level of HeII, 7 levels of C and 1 level of CII, 7 levels of SiI and 1 level of SiII, 5 levels of Mg I and 1 level of MgII, 4 levels of AlI and 1 level of Al II as potential photo-ionization contributors and the following abundances to mimic the abundances in HgMn stars: 0.06 for He (H = 1.0), 1.5×10^{-4} for C, 1.1×10^{-4} for N, 6.7×10^{-4} for O, 7.9×10^{-6} for Mg, 2.3×10^{-7} for Al, 3.5×10^{-5} for Si; and 6.3×10^{-6} and 6.3×10^{-8} for Ga respectively.

CCP7 software (Tlusty, Synspec) was used to produce models with recalculated hydrostatic equilibrium and to produce NLTE level populations and detailed line profiles. The codes, however, deal with elements up to 30 and were slightly modified to study the gallium. Particularly, the code Tlusty produces NLTE model atmosphere under radiative, hydrostatic and statistical equilibria with the hybrid complete linearization/ALI methods. The overall maximal relative change of all model physical quantities and level populations was required to be 0.01 in every depth point.

7. Rates in rate equations

The statistical equilibrium is usually reached through rate equations, i.e. for element with explicit levels, where rate equation describes the creation-destruction balance for level. The rate equation are written in classical form as

$$n_i.\sum p_{ij} - \sum n_j.p_{ji} = 0 \qquad (2)$$

where the total transition probability p_{ij} consists from radiative rates R_{ij} of the ij transition and collisional rates C_{ij} and n stands for level population. To identify the processes Table 2 offers ratio of rates: collisional rates (col) in ID depth point vs. maximal depth point ID = 64 (where LTE is fulfilled), the same for radiative de-excitation rate (d) and the ratio of radiative excitation and de-excitation rates (u/d) in ID point. Depth point of stellar atmosphere is identified both by ID number and logarithm of mass-depth-variable quantity (DM). The table corresponds to the effective temperature 13 000 K, the surface gravity $\log g = 4$, the abundance $A_{\rm Ga} = 6.3\times10^{-6}$ model and the abundace $A_{\rm Ga} = 6.3\times10^{-8}$ does not change the values of rates in the case of our model atmosphere.

Table 3. Gallium transitions equivalent widths [mÅ].

Transition	log gf[1]	lte[2]	nlte	lte[2]	nlte
GaI2945	0.07	21.5	16.2	0.4	0.3
GaII1414	0.25	1811.5	1614.1	192.7	173.0
GaII4262	0.97	49.6	46.1	2.8	2.5
GaII6334	0.36	29.6	20.4	0.9	0.4
GaIII1534	–0.24	656.0	530.6	94.1	81.4
GaIII1495	0.05	937.9	894.9	119.7	113.7

[1] VALD database (Piskunov et al. 1995).
[2] $A_{\rm Ga} = 6.3\times10^{-6}$ and 6.3×10^{-8}.

8. Departure coefficients, level populations and total source function

In this section we will discuss the level population for gallium, NLTE departure coefficients, total source function as well as all associated physical processes. The common feature for all departure coefficients is to decrease towards the stellar surface (i.e. lower depth-mass-variable value). Naturally, the levels are in most cases underpopulated. The LTE and NLTE equivalent widths (in mÅ) are given in Table 3. Figure 2 displays departure coefficients for

lower and upper levels for GaII 1414 Å and 6334 Å lines and hydrogen line as well (for comparison). The resultant hydrogen NLTE profile is easy to explain, the departure coefficients are less than unity (∼0.2 in log scale). Even the level population for lower level differs owing to the upper one and the NLTE source function differs from the LTE one, the overall profile changes little as well as the NLTE equivalent width. Remarkably, the changes in radiative and collisional rates (against bottom part of the atmosphere and implicitly LTE option, Table 3) are competitive upwards to the atmosphere. The line core is dominated out of equilibrium, the spontaneous de-excitations exceeds the excitation by about 30% where also the largest NLTE effect can be expected.

The level populations for 1414 Å transition are more strongly underpopulated, the departure coefficients reach the value up to –3 (in log scale). In addition, the coefficients has similar behaviour, thus the total NLTE line source function

$$S = \frac{2h\nu^3}{c^2}.\left(\frac{g_j b_i}{g_i b_j} - 1\right)^{-1} \quad (3)$$

where b_i and b_j are departure coefficients, changes little with respect to the LTE one, however since the line absorption coefficient is weighted (Eq. (1)) by the b_i factor and since b_i factor works equivalently as the abundance, we can expect smaller NLTE equivalent width.

The 6334 Å transition is similar, the departure coefficients are of similar behaviour reaching the values down to –2.

9. Fine structure

The gallium model atom does not take into account fine structure since close energy states were lumped together. Now such a model atom is not too difficult to build up and make computations, but we investigate qualitatively this effect. Firstly, the common feature of departure coefficients is to decrease towards the stellar surface. Secondly, the 1495 Å and 1534 Å gallium transitions have close upper energy levels while the departure coefficients are almost identical. Thirdly, the common process in gallium is the de-population and collisional rates in rate equations are in many cases important.

We have from the above discussion that the NLTE level populations should not differ in fine structure levels and the problem is restricted either to the LTE level populations and including fine structure in LTE calculations (see again Dworetsky et al. 1998 for example) or to consider the NLTE level population and treat all levels the same.

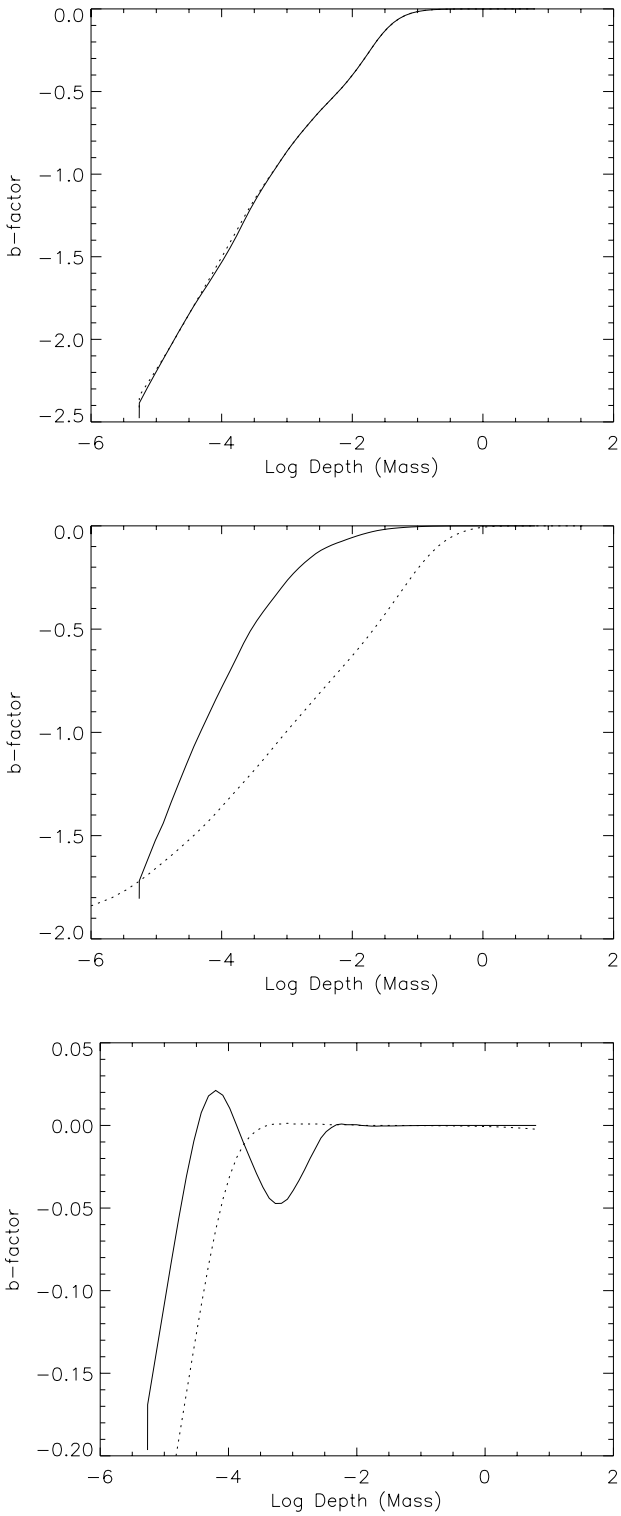

Fig. 2. GaII1414 (upper panel), 6334 (mid panel) and Hγ (bottom panel) NLTE departure coefficients. Log–log diagram of the departure coefficient (b-factor) vs. mass-depth-variable (g/cm^2). Legend: **solid** line –lower level and **dotted** line – upper level, $A_{\rm Ga} = 6.3 \times 10^{-6}$.

10. Conclusions

This work is an improvement on earlier calculations by Zboril (1997) and as such they represent the first detailed look at NLTE for gallium. Given the temperature structure from LTE models for early type stars and properly recalculated hydrostatic equilibrium with the abundances suitable for a CP3 star we evaluated NLTE level

populations for most prominent gallium transitions as identified in real spectra with the following results:

1. the common feature of departure coefficients is to decrease towards the stellar surface. This starts at the depth point of visual continuum forming region (log DM ∼–1) for most transitions;
2. the collisional rates in equations for statistical equilibria in transitions are larger (about 1 dex) in comparison with radiative rates, except for the 1414 Å transition;
3. the global NLTE effect starts already at depths of the visual continuum forming region: both collisional and radiative rates are reduced dramatically (up to 10%) with respect to the values valid for maximal depth point where LTE is assumed. In particular, for most transitions the strong spontaneous de-excitation occur when the excitation balance is away from LTE treatment but only for the very high atmosphere part (ID = 10). This might influence only the strongest transitions (1414, 1495 and perhaps 1534);
4. under the LTE approach the abundances derived from UV lines are underestimated by about 0.15 dex and from optical lines by about 0.1 dex. The results show that NLTE considerations reduce the discrepancy between UV and optical abundances (0.22 from Dworetsky et al. 1998) slightly, claiming further reduction of 0.1 dex from use of detailed hyperfine structure, the discrepancy is reduced to about 0.05 dex and it may be resolved by more accurate atomic parameters.

Finally, we wish to stress that modified CCP7 software (plus test run files) are available in compressed *tar* form and can be uploaded upon request to the authors, either to repeat the computations or to extend (the ranges of $T_{\rm eff}$, $\log g$ etc.). Also this theoretical approach attempts to study processes in gallium transitions (if the transition is controlled by collisions, photoionization, level population and de-population processes, to estimate NLTE equivalent width) rather than make abundance analysis for a set of HgMn stars using real spectra. This can be done upon request and/or by Tlusty software users.

Acknowledgements. The UK Research Council's Collaborative Computational Project 7 (CCP7) is gratefully acknowledged. MZ also wishes to acknowledge some assistance of M. J. Seaton and M. M. Dworetsky. This work was partially supported by grant No. 2/1024/21 of Grant Agency for Science. We thank the anonymous referee for valuable comments.

References

Adelman, S. J. 1998, A&AS, 132, 93
Babel, J., & Montmerle, T. 1997, A&A, 323, 121
Berrington, K. A., Eissner, W. B., & Norrington, P. H. 1995, Comput. Phys. Commun., 92, 290
Budaj, J., Zboril, M., Zverko, J., Žižňovský, J., & Klačka, J. 1993, ASP Conf. Ser., 44, 502
Drake, S. A., Linsky, J. L., Schmitt, J. H. M. M., & Rosso, C. 1994, ApJ, 420, 387
Dworetsky, M. M., Jomaron, C. M., & Smith, C. A. 1998, A&A, 333, 665
Hubeny, I., Lanz, T. & Jeffery, C. S. 1994, CCP7 User Guide
Jomaron, C. M., Dworetsky, M. M., & Allen, C. S. 1999, MNRAS, 303, 555
Kurucz, R. L. 1979, ApJS, 40, 1
Landstreet, J. D. 1982, ApJ, 258, 639
Lanz, T., Artru, M.-C., Didelon, P., & Mathys, G. 1993, A&A, 272, 465
Michaud, G. 1970, ApJ, 160, 641
Michaud, G. 1981, in Upper Main Sequence Chemically-Peculiar Stars, 23rd Liege Astrophys. Coll., ed. P. Renson, 355
Michaud, G. 1986, IAU Coll., 90, 459
Piskunov, N. E., Kupka, F., Ryabchikova, T. A., Weiss, W. W., & Jeffery, C. S. 1995, A&AS, 112, 525
Smith, K. C., & Dworetsky, M. M. 1993, A&A, 274, 335
Smith, K. C. 1994, A&A, 291, 521
Smith, K. C. 1995, A&A, 297, 237
Smith, K. C. 1996, A&A, 319, 928
Smith, K. C. 1997, A&A, 305, 902
Takada-Hidai, M., Sadakane, K., & Jugaku, J. 1986, ApJ, 304, 425
Woolf, V. M., & Lambert, D. L. 1999, ApJ, 521, 414
Zboril, M., & Budaj, J. 1993, Inf. Bull. on Var. Stars, No. 3913
Zboril, M. 1997, Ph.D. Thesis
Zboril, M., & Budaj, J. 1999, Inf. Bull. on Var. Stars, No. 4748